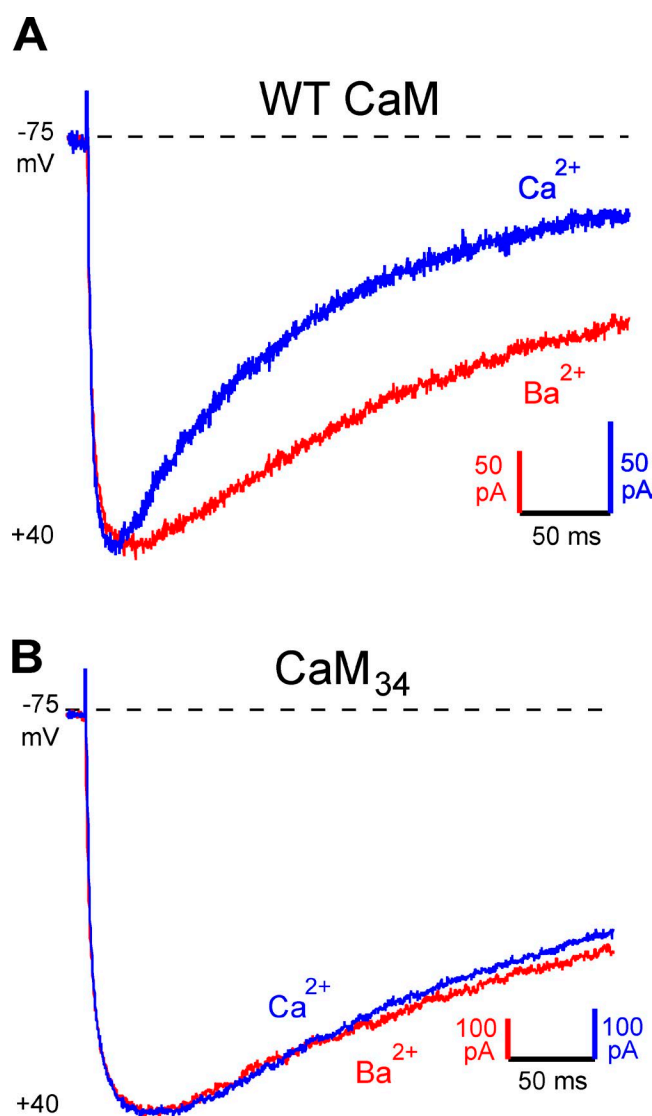
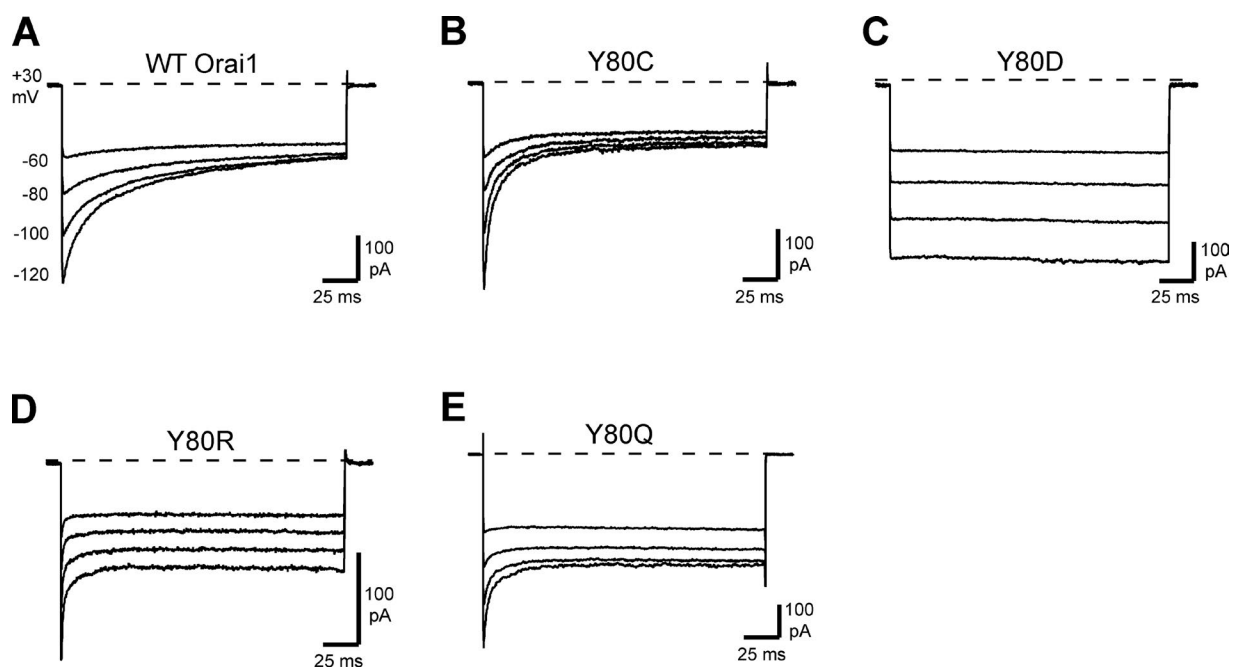
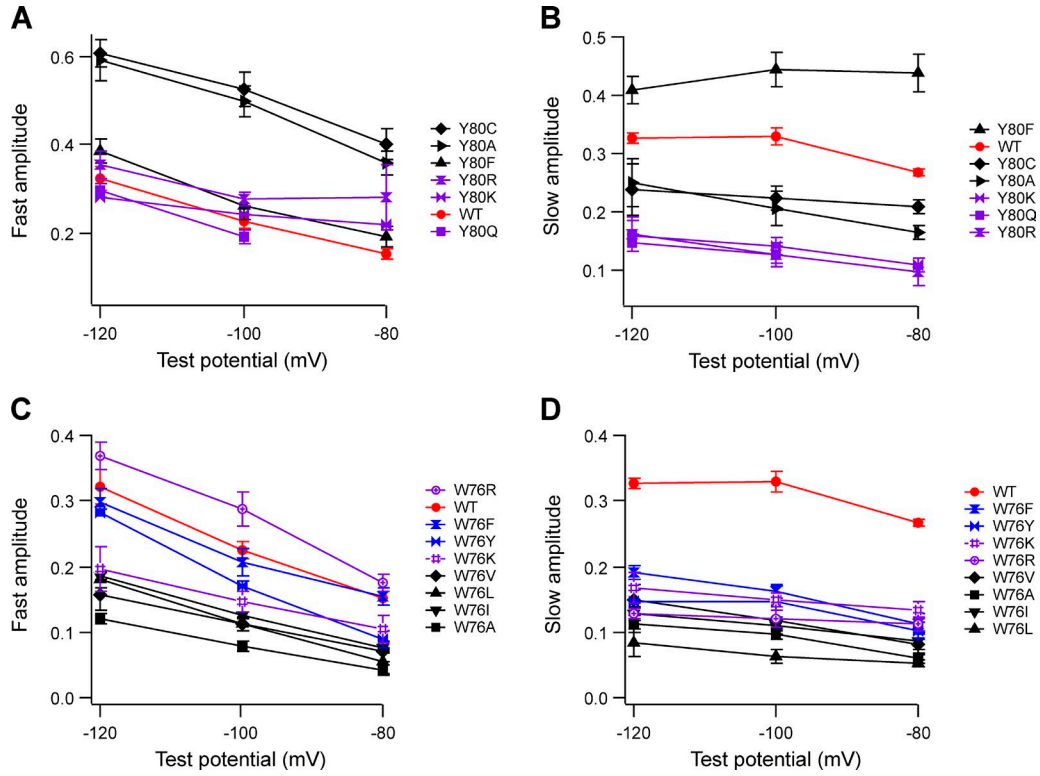


Mullins et al., <http://www.jgp.org/cgi/content/full/jgp.201511437/DC1>

**Figure S1.** CDI of  $\text{Ca}_v1.2$  currents is suppressed by  $\text{CaM}_{34}$ . HEK293H cells were transfected with  $\text{Ca}_v1.2$ ,  $\beta 1b$ ,  $\alpha 2\delta 1$ , and  $\text{CaM}$ -IRES-GFP and recorded during 300-ms depolarizing steps from a holding potential of  $-75$  mV (see Materials and methods). (A) Representative scaled currents in  $20$  mM  $\text{Ca}^{2+}$  (blue) and  $20$  mM  $\text{Ba}^{2+}$  (red) recorded from a single cell transfected with WT  $\text{CaM}$  and stepped to  $+40$  mV. The difference between the blue and red traces is a measure of CDI, and the remaining inactivation in  $\text{Ba}^{2+}$  is by definition voltage-dependent. (B) Representative scaled currents in  $20$  mM  $\text{Ca}^{2+}$  (blue) and  $20$  mM  $\text{Ba}^{2+}$  (red) recorded from a single cell transfected with  $\text{CaM}_{34}$  and stepped to  $+40$  mV. The similarity of the scaled traces in  $\text{Ca}^{2+}$  and  $\text{Ba}^{2+}$  is consistent with almost complete suppression of CDI by  $\text{CaM}_{34}$ . The current remaining at the end of the pulse was divided by the peak current to obtain a normalized measure of inactivation for each cell in both  $\text{Ca}^{2+}$  and  $\text{Ba}^{2+}$  ( $R_{300}$  for  $\text{Ca}^{2+}$  and for  $\text{Ba}^{2+}$ ). For summary and statistical comparisons, the difference between the  $R_{300}$  values in  $\text{Ca}^{2+}$  vs.  $\text{Ba}^{2+}$  ( $\Delta R_{300}$ , an index of CDI) was determined for each cell at several potentials, and the mean  $\pm$  SEM for  $n = 4$ – $5$  cells from each condition are plotted in Fig. 2 A (bottom).



**Figure S2.** Representative currents for additional mutations at Orai1 position Y80. All currents were recorded and analyzed as described for Fig. 3. Representative currents are shown for WT Orai1 (A, same traces shown in Fig. 3 A) and the Orai1 point mutants Y80C (B), Y80D (C), Y80R (D), and Y80Q (E). Extents of CDI for these mutations are summarized in Fig. 3 G. Fast and slow time constants from bi-exponential fits are plotted against test potential in Fig. 3 (H and I) and fast and slow component amplitudes are summarized in Fig. S3 (A and B).



**Figure S3.** Fast and slow contributions to CDI for Orail mutations at the Y80 and W76 positions. (A–D) Current traces collected in 20 mM  $\text{Ca}^{2+}_o$ , were fitted by the biexponential function  $I = I_o + A_1 e^{-t/\tau_1} + A_2 e^{-t/\tau_2}$ , where  $\tau_1$  and  $\tau_2$  represent fast and slow time constants. Time constants from these fits are included in Figs. 3 and 5. Each point represents the mean  $\pm$  SEM for  $n = 4$ –7 cells. Fast (A) and slow (B) amplitudes for Y80 mutations are plotted against test potential. Fast (C) and slow (D) amplitudes for W76 mutations are plotted against test potential.

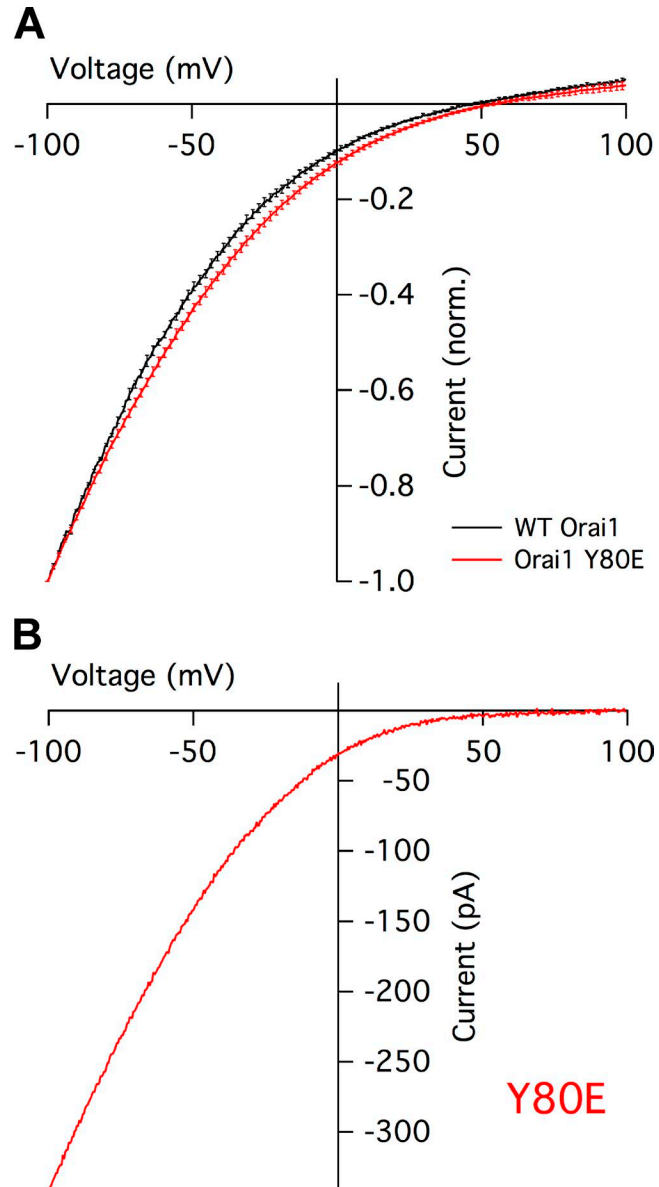


**Figure S4.** Selectivity of the Orail Y80E mutant channels as assessed by voltage ramps. (A) WT and Orail Y80E mutant currents were measured in DVF external solution during 100-ms hyperpolarizing steps to  $-100$  mV (not depicted) followed by 100-ms ramps from  $-100$  mV to  $+100$  mV. Data were leak-subtracted and normalized to the current at  $-100$  mV. Normalized mean  $\pm$  SEM (with SEM plotted for every fifth point) is shown for  $n = 5$  cells. (B) Orail Y80E current evoked in  $20$  mM  $\text{Ca}^{2+}$  Ringer's solution by the step-ramp protocol described in A (mean of five consecutive leak-subtracted ramp currents from a representative cell).

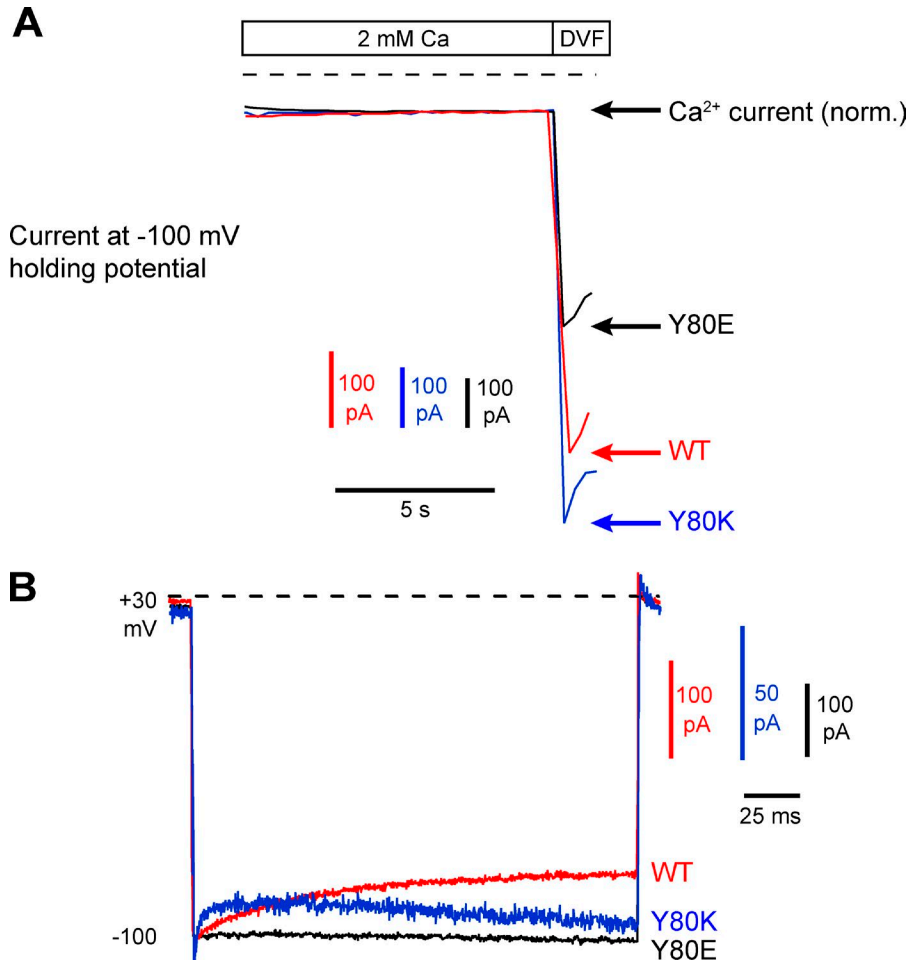


**Figure S5.** A method for estimating  $i_{Ca}$  from  $i_{Na}$ . We estimated the unitary Ca<sup>2+</sup> current ( $i_{Ca}$ ) using the following equation (see Materials methods):

$$i_{Ca} = i_{Na} \frac{I_{Ca}}{I_{Na}} \frac{1}{(1 - CDI)},$$

where  $I_{Ca}$  is the Ca<sup>2+</sup>-CRAC current measured in 2 mM Ca<sup>2+</sup>,  $I_{Na}$  is the Na<sup>+</sup>-CRAC current measured immediately after switching to DVF extracellular solution, and  $CDI$  is the extent of inactivation in 2 mM Ca<sup>2+</sup> at -100 mV. Dashed lines indicate zero current level. (A) Measuring  $I_{Ca}$  and  $I_{Na}$ . Scaled representative currents are shown for WT (red), Y80K (blue), and Y80E (black) Orai1 channels recorded at -100 mV holding potential starting in 2 mM Ca<sup>2+</sup> (top arrow), and the color-coded arrows mark the peak currents attained upon switching to DVF. Mean  $I_{Ca}/I_{Na}$  values were  $0.096 \pm 0.005$  (WT,  $n = 3$ ),  $0.082 \pm 0.009$  (Y80K,  $n = 4$ ), and  $0.156 \pm 0.007$  (Y80E,  $n = 4$ ). (B) Measuring the CDI correction factor. Scaled representative currents from WT (red), Y80K (blue), and Y80E (black) channels are shown during 200-ms pulses from +30 to -100 mV in 2 mM Ca<sup>2+</sup>. The current remaining at 195 ms was divided by the peak current 1–3 ms after the beginning of the pulse. For Y80K channels, which showed slow potentiation in 2 mM Ca<sup>2+</sup>, the minimum current during the pulse was used. The values of remaining current were averaged from four cells, and the inverse ( $1/(1 - CDI)$ ) was used as a CDI correction factor to compensate for the partial inactivation of Ca<sup>2+</sup> current that is immediately lost upon exposure to DVF. The CDI correction factors were 1.27 (WT), 1.11 (Y80K), and 0.99 (Y80E).

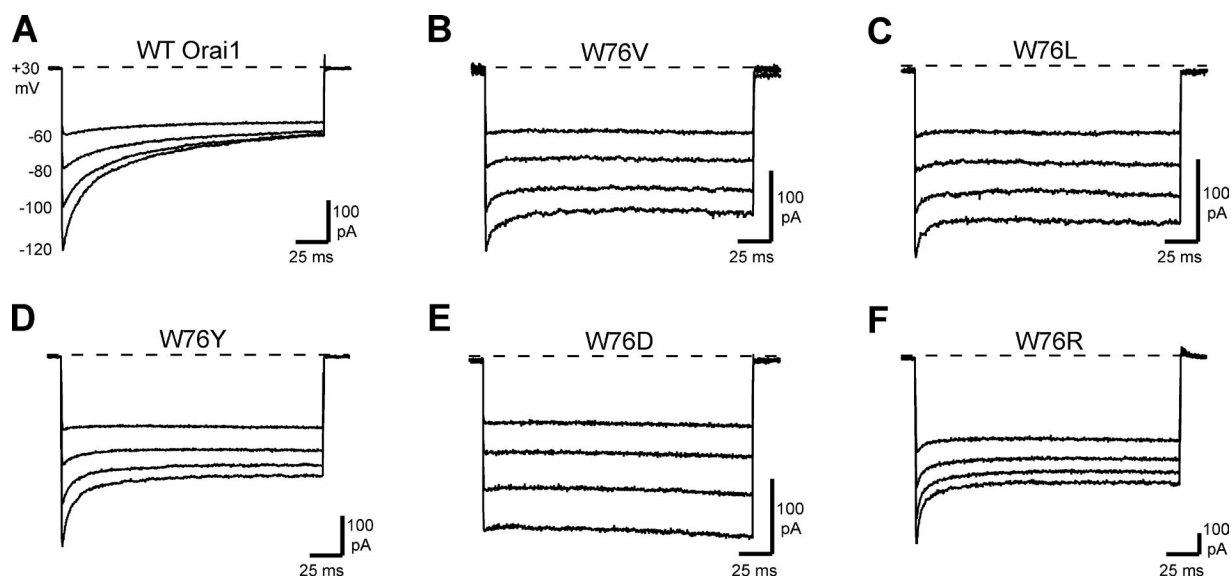


**Figure S6.** Representative currents for additional mutations at Orail position W76. All currents were recorded and analyzed as described for Fig. 3. Representative currents are shown for WT Orail (A, same traces shown in Fig. 3 A) and Orail point mutants W76V (B), W76L (C), W76Y (D), W76D (E), and W76R (F). Extents of CDI for these mutations are summarized in Fig. 5 G. Fast and slow time constants from biexponential fits are plotted against test potential in Fig. 5 H and I. Corresponding amplitudes of fast and slow components are summarized in Fig. S3 (C and D).

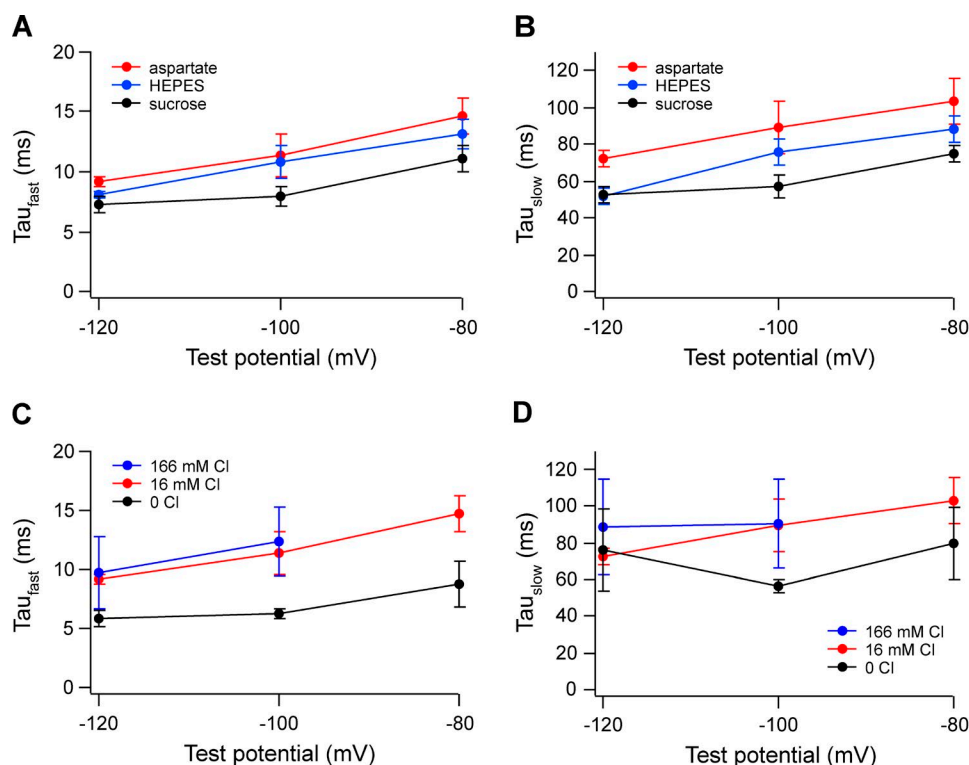


**Figure S7.** Inactivation kinetics for WT Orail with a range of internal anions. (A–D) Current traces like those shown in Fig. 7 were fitted by the biexponential function  $I = I_o + A_1 e^{-t/\tau_1} + A_2 e^{-t/\tau_2}$ , where  $\tau_1$  and  $\tau_2$  represent fast and slow time constants of inactivation. Each point represents the mean  $\pm$  SEM for  $n = 5$ –6 cells. Fast (A) and slow (B) time constants of inactivation for aspartate, HEPES, and sucrose are plotted against test potential. Fast (C) and slow (D) time constants of inactivation for three chloride concentrations are plotted against test potential.